Towards the establishment of weldability test standards for hydrogen-assisted cold cracking

R. Kurji · N. Coniglio

Abstract Industry and research have long desired the establishment of standards for weldability testing in regards to hydrogen-assisted cold cracking formation. This would have the obvious advantage of allowing data to be reliably compared between different research labs. But making decisions regarding standards requires some careful thought and agreement on i) how test parameters affect test results, ii) what exactly needs to be measured, and iii) how test results should be interpreted and reported. Our depth of understanding on these points has matured significantly over time and, while there is not always universal agreement, it is at least possible to start highlighting factors important to standards. This paper examines these factors, including the welding parameters, restraint, hydrogen, and cracking index. When comparing different alloys having different thermal characteristics, the use of constant welding parameters (common practice) will result in variable weld penetration and weld pool shape, which can influence grain shape and microstructural features, which can result in inequitable weldability comparisons. Welding on test coupons having different dimensions can affect restraint, which will influence the residual stresses around the weldment. High restraint usually results in higher crack susceptibility. Also, hydrogen content present in a weldment depends on the thermal history, welding parameters, and surrounding atmosphere humidity, with high hydrogen contents associated to great cracking susceptibility. Finally, the selection of an appropriate cracking index is required for data analysis. Quantifications of crack length and minimum preheat temperature are common indexes used for comparison. Critical stress and hydrogen content are other indexes. But how well these indexes actually represent weldability are contentious issues. This paper will examine and quantify these issues in detail, thus providing the reader with an appreciation of all things that must be considered when preparing a standardized procedure for weldability testing.

Keywords Weldability tests · Restraint · Stress · Welding parameters · Hydrogen-assisted cold cracking

Nomenclature

CTS	Controlled thermal severity
FCAW	Flux-cored arc welding
G-BOP	Gapped bead-on-plate
GMAW	Gas metal arc welding
HACC	Hydrogen-assisted cold cracking
HAZ	Heat-affected zone
IG	Intergranular
IRC	Instrumented restraint cracking
MVC	Macrovoid coalescence
M-WIC	Modified Welding Institute of Canada
QC	Quasi-cleavage
RRC	Rigid restraint cracking
SAW	Submerged arc welding
SMAW	Shielded metal arc welding
TRC	Tensile restraint cracking
WIC	Welding institute of Canada
WM	Weld metal

1 Introduction

The establishment of a standardized weldability test for hydrogen-assisted cold cracking (HACC) is an ongoing topic

R. Kurji
School of Mechanical Engineering, The University of Adelaide, Adelaide, Australia

N. Coniglio (✉)
MSMP Laboratory, Arts et Metiers ParisTech, 2 cours des Arts et Metiers, 13617 Aix en Provence, France
e-mail: nicolas.coniglio@ensam.eu

of interest for the industry. This would have the obvious advantage of enabling a reliable comparison in cracking susceptibility between diverse alloys and welding conditions. Cracking is generally believed to result from the tensile fracture at room temperature of a hydrogenated solid metal.

Significant work has already been devoted to characterize weldability [1–5]. In addition, there is no huge disparity found in alloy rankings between different tests and laboratories [6]. In addition, there does not appear to be a large disparity between test rankings and perceived real-world behaviour [3, 6]. However, even though the numerous existing tests appear to do a reasonable job of providing a rough comparison (i.e. ranking) of alloy weldability, the problem arises in not knowing how variations in testing procedure may affect test rankings and how test results relate to real welding applications. Difficulty may be encountered in deciphering small differences in weldability between similar alloys. There is also the inability to predict, with any certainty, whether or not cracking will occur in a specific application. This has led one to question the validity of these trends, if tests are being performed correctly, or if the correct things are being measured. In essence, this begs a bigger question of how test measurements actually relate to weldability.

Full-scale testing [4, 6] has been adopted in an effort to bypass the difficulties inherent in predicting field behaviour from small-scale laboratory tests. However, due to the complexity and large dimensions of full-scale testing, smaller-scale restraint cracking tests have been developed to evaluate the weldability in laboratories, limiting the full-scale weldability tests to a validation role of in-field welding procedure. Nevertheless, limitations exist in providing an overview of the alloy's weldability. The broad spectrum of loading methods (e.g. load orientation, tension, or bending) and weldability test design (shape, size) bring about inconsistencies in the testing methodology and collected data. These discrepancies highlight a lack of understanding and agreement on the critical variables controlling crack formation.

The goal of the present paper is to provide a perspective on establishing future standards for the weldability testing of different alloys and welding conditions. A review of the status of current weldability testing in the literature is compiled to identify important test parameters and test limitations. The meaning behind weldability data is examined. A checklist summary is provided that facilitates the comparison of weldability data.

2 Alloy composition

When considering weldability, minute details regarding alloy composition and impurities can be of utmost importance. For this reason, it is necessary to accurately measure and document base metal, filler metal, and weld metal compositions. Certain alloy systems are notorious for poor weldability, and so both base metal and filler metal compositions should always be determined and reported. For flux-based welding processes (for example cellulosic SMAW [7] and SAW [8] processes), flux chemistry can likewise have a major effect on weld metal composition and subsequently affect the crack susceptibility of the weld metal [9]. Experimental G-BOP test data have even shown that base metal compositions can also influence the weld metal crack susceptibility for small filler dilutions [10]. Possibilities for inadvertent weld contamination must also be considered, including shielding gas, joint preparation, weld fixtures, and entrained weld spatter. Outlined below are two characteristic features that demonstrate the importance of alloy composition on weldability.

2.1 Carbon equivalent

The steel-based systems that are welded today represent a broad spectrum of steel compositions, rendering a direct comparison difficult. Thus, carbon equivalent formulas have been developed to provide a quantitative value representative of the weldment composition [11, 12]. This value has in turn served as a proxy to cracking susceptibility. Several empirical values have been proposed (Table 1) weighting each element's effect in regards to the reference element carbon [13–20]. Hence, these formulas are usually limited in a range of compositions that are included into the envelope of compositions used for their determination. The P_{cm} value has been estimated as a better crack susceptibility index [11], but this remains a highly contentious subject as high P_{cm} values are not necessarily associated to high crack susceptibility [21]. As none of the existing carbon equivalent formulas seems suitable to evaluate the critical preheat temperature required in weld metal steels to avoid cracking [11], the welding conditions can be converted into CEN increments to account for the welding conditions [22]. Nevertheless, the general trend follows the carbon content–carbon equivalent mapping concept as designed by the Graville diagram (Fig. 1), where maximum crack susceptibility happens for simultaneously high carbon contents and high carbon equivalent values (zone III in Fig. 1).

2.2 Solidification mode

The location of the cracking in high strength low alloy steel weldments has been shown to be controlled partly by the solidification mode (determined by alloy content) [23]. The hydrogen solubility drops during the primary austenite-to-ferrite transformation and diffuses to the adjacent austenitic zones (Fig. 2). As the used base metals have higher strengths, the required strength matching between the weld metal and base metal is achieved by the use of richer electrode chemistries, thus delaying in time the weld metal austenite-to-ferrite transformation and enhancing hydrogen transportation from

Table 1 Carbon equivalent formulas and their applicability

Carbon equivalent formula	Application range according to Talas et al. [11]	Application range according to Yurioka et al. [3]	Reference
Group A			
$CE_{IIW} = C + \frac{Mn}{6} + \frac{Ni+Cu}{15} + \frac{Mo+V}{5}$	C-Mn steels with high CE content	$C \leq 0.08$ %	13
$CE_{WES} = C + \frac{Si}{24} + \frac{Mn}{6} + \frac{Ni}{40} + \frac{Cr}{5} + \frac{Mo}{4} + \frac{V}{14}$			14
Group B			
$CE_{DNV} = C + \frac{Si}{24} + \frac{Mn}{10} + \frac{Ni+Cu}{40} + \frac{Cr}{5} + \frac{Mo}{4} + \frac{V}{10}$	Steels with lower CE contents	$0.08\ \% \leq C \leq 0.12\ \%$	15
$CE_T = C + \frac{Mn}{10} + \frac{Cu}{20} + \frac{Ni}{40} + \frac{Cr}{20} + \frac{Mo}{10}$			16
Group C			
$Pcm = C + \frac{Si}{30} + \frac{Mn}{20} + \frac{Cu}{20} + \frac{Ni}{60} + \frac{Cr}{20} + \frac{Mo}{15} + \frac{V}{10} + 5B$	Pipeline steels	C ≤0.12 %	17
$CE_{PLS} = C + \frac{Si}{25} + \frac{Mn}{16} + \frac{Cu}{16} + \frac{Ni}{60} + \frac{Cr}{20} + \frac{Mo}{40} + \frac{V}{15}$			18
$CE_{HSLA} = C + \frac{Mn}{16} - \frac{Ni}{50} + \frac{Cr}{23} + \frac{Mo}{7} + \frac{Nb}{5} + \frac{V}{9}$			19
Group D			
$CE_N = C + f(C) * \left(\frac{Si}{20} + \frac{Mn}{6} + \frac{Cu}{15} + \frac{Ni}{20} + \frac{Cr+Mo+Nb+V}{5}\right)$ $f(C)=0.75+0.25\tanh[20(C-0.12))]$	All steels	$C \leq 0.3$ %	20

HAZ to weld metal. This explains the trends towards the greater likelihood of crack formation in the weld metal nowadays.

3 Test selection

Selecting the most appropriate weldability test requires careful consideration of many different aspects including cost, availability, and type of cracking expected. Because tests are typically not available commercially, this requires in-house design and construction, leading to unique test variations from one laboratory to another. Test designs can vary in complexity from a simple turn-table to make a restraint circular weldability test (cost ≈US$1K) to a variable speed tensile restraint cracking test (≈US$100K). Some tests have the restraining support integrated into the specimen design, requiring its fabrication for each test sample.

3.1 Type of tests

A broad variety of weldability tests has been developed over the years. Their designs impose controlled restraint and/or stress–strain after welding in the weldment region [5]. Table 2 lists different weldability tests according to classifications discussed below.

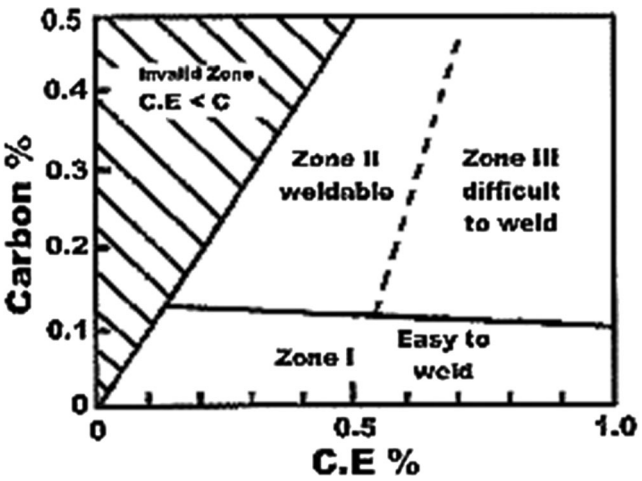

Fig. 1 Graville diagram demarking regions for cracking applied to steels

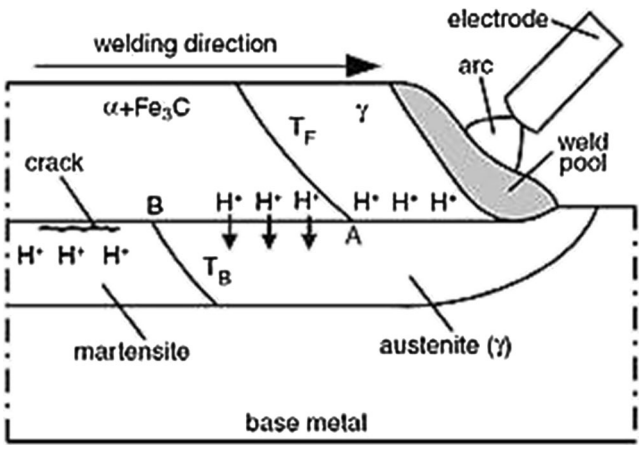

Fig. 2 Schematic illustration of hydrogen diffusion in steels [23]

Table 2 Overview of weldability tests developed for characterizing weld metal susceptibility to HACC

Test	Intrinsic vs extrinsic	Bending vs tensile	Longitudinal vs transverse loading	HACC cracking index	Reference
One-side lifted pipe	Extrinsic	Bending	Transverse	Crack length lifting height	4
Four-point bending pipe	Extrinsic	Bending	Transverse	Crack length bending force	6
Cranfield test	Intrinsic	Tensile	–	Crack length	3
WIC test	Intrinsic	Tensile	Transverse	Restraint preheat	6, 9, 24, 25
M-WIC test	Intrinsic	Tensile	Transverse	Restraint preheat	26
Implant test	Extrinsic	Tensile	Transverse	Stress	21, 25, 27–30
t test	Intrinsic	Tensile	Transverse	Crack length	3
Bending test	Extrinsic	Bending	Transverse	Crack length deflection	31–33
Tensile restraint cracking TRC test	Extrinsic	Tensile	Transverse	Load	3
Rigid restraint cracking RRC test	Extrinsic	Tensile	Transverse	Load strain restraint	34
Window-type cruciform restraint test	Intrinsic	Tensile	–	Crack length	3
Controlled thermal severity CTS test	Intrinsic	Tensile	–	Cooling rate	35
Gapped bead-on-plate G-BOP test	Intrinsic	Tensile	Longitudinal	Crack length	10, 36–38
One-plate self-restraint weldability test	Intrinsic	Tensile	Transverse	Crack length preheat	4
Restraint circular weldability test	Intrinsic	Tensile	Transverse	Crack length	3
Lehigh U-groove, or Stout, test	Intrinsic	Tensile	Transverse	Crack length	4
Lehigh slot test	Intrinsic	Tensile	Transverse	Crack length	29, 39
Tekken test, or y-groove restraint test	Intrinsic	Tensile	Transverse	Hydrogen content preheat	40
Instrumented restraint cracking IRC test	Intrinsic	Tensile	Transverse	Crack length	3
Restraint root cracking test, or Schnadt-Fisco test	Intrinsic	Tensile	Transverse	Crack length	6
H-slit restraint test	Intrinsic	Tensile	Transverse	Crack length	3
Window-type restraint multiple-layer cracking	Intrinsic	Tensile	Transverse	Crack length restraint	41

3.2 Intrinsic vs extrinsic

Intrinsic tests rely upon internally generated stresses and strains to cause cracking. While simple and less expensive to perform, intrinsic tests typically involve complex and non-uniform loading that evolve during cooling and cannot be easily quantified. This limits the collection of information that would help define critical conditions needed for cracking. Even so, these tests provide an easy and inexpensive way to rank alloys, if that is all that is desired. The severity of loading can often be systematically varied, for example, by changing coupon dimensions, slot depths (Lehigh test), restraint distance (WIC and M-WIC tests), or circle diameter (restraint circular weldability test). A detracting aspect of these tests is the difficulty in separating out effects of welding parameters and material properties, since the stress/strain experience is strongly linked to these values.

Extrinsic tests, on the other hand, involve the controlled application of an external stress or strain during welding that enables loading to be more independent of material properties or welding parameters. These tests are more expensive to build, but allow for the quantification of loading and/or straining. The simplest of these tests is the bending test [31–33]. More complicated but popular in the 80s, the implant test [21, 25, 27–30] investigates the cracking characteristics of HAZ region, but its difficult reproducibility (such as implant location) and its unusual load field make it difficult to transfer the data to in-field applications.

Intrinsic and extrinsic tests differentiate in the stress evolution as the crack propagates [29], as indicated in Fig. 3 with

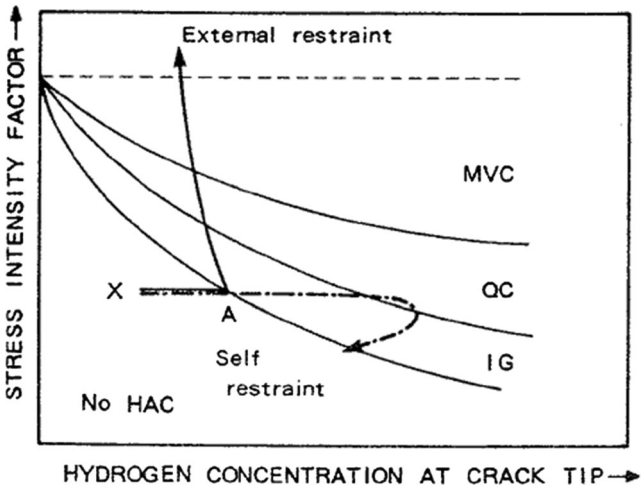

Fig. 3 Superposition on Beachem diagram of stress history at crack tip (indicated by *lines* with *arrows*) for external loading and self-restraint cracking tests [3]

the stress history superimposed on Beachem diagram. While the load drops with crack opening in an intrinsic test, the extrinsic test that maintains a constant loading value generates an increase in stress intensity as the crack size grows. The reduced threshold hydrogen content required for crack growth correlates to the increased stress intensity at the crack tip and subsequent macrovoid coalescence (MVC) fracture mode. Thus, intrinsic tests provide through their stress relief access to critical conditions for crack arrest. With the concept illustrated in Fig. 3, the cracking mode (MVC, QC, IG) provides post-mortem indications on the stress intensity value that induced crack growth.

3.3 Bend vs tensile

Bend-type extrinsic tests [31–33] apply controlled strain to a weld by forcing a specimen to conform to the surface radius of a die block (Fig. 3). Hence, the maximum strain experienced in the vicinity of the weldment (ε in mm mm^{-1}) is determined by the radius of curvature of mandrel (R in mm) and the specimen thickness (t in mm):

$$\varepsilon = \frac{t}{2R} \times 100\% \quad (1)$$

Mandrels having different radii can be exchanged in a series of tests to vary the maximum applied strain. A minimum amount of strain is needed to get cracking depending upon the material and is observed by a sudden drop in the applied force. The weld specimen is either kept at low temperatures to immobilize hydrogen prior to testing [2] or machined from the initial weld 24 h after the weld completion [32, 33]. The former method must be applied with care as microstructural changes may occur at low temperatures. The latter method consists of using the bending test as an opener of pre-existing cracks to facilitate their observation and counting. The bending is carried out at room temperature and slow loading rates to maximize the hydrogen embrittling effects. The formation of a significant number of cracks is indicated by a load drop on the load-deflection curve [2]. The bend-type tests have also been used to open pre-cracked welds to facilitate crack counting (Fig. 4).

While bending tests are easy to perform, they do not lend themselves to the precise determination of critical conditions needed for cracking. The non-uniform distribution of strain and strain rate within the coupon during strain application varies over the duration of the test and throughout the coupon thickness. “Hinging” is another problem that can occur in bend tests, arising from the non-conformity of the specimen with the die block as depicted in Fig. 5, where plastic deformation is concentrated in hot material along the weld seam.

Cross-weld tensile tests in comparison are much better suited for measuring critical values of strain and strain rate needed for cracking. Specifically, it is advantageous to have the direction of loading oriented perpendicular to weld metal centre-line grain boundaries. At any point in time, the load, strain, and strain rate are uniform through the coupon thickness for full-penetration welds.

3.4 Guidance for crack location

Hydrogen-assisted cold cracking may form in the HAZ or weld metal depending on metallurgical features, hydrogen distribution, loading, and groove design. The implant test [21, 25, 27, 28] investigates the cracking susceptibility of the only HAZ by loading a pre-placed implant over which a butt weld was deposited (Fig. 6), but the reproducibility of the implant location within the HAZ is difficult. Other tests control the stress in the vicinity of the weldment in part through the shape of the welding groove. A U-groove (Lehigh U-groove test) favours crack formation at the root of the weld metal rather than in the HAZ while a y-groove (Tekken test) facilitates the cold cracking in the HAZ of the root of the weldment [3, 4].

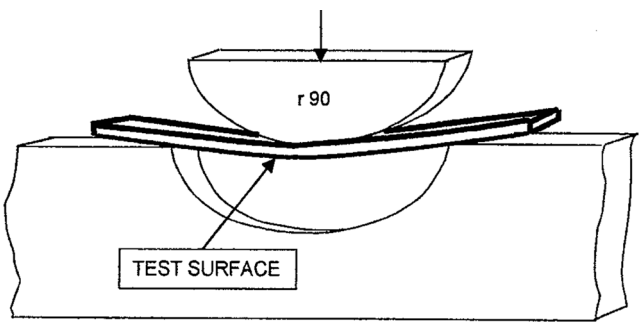

Fig. 4 Experimental setup of bending weldability test [32]

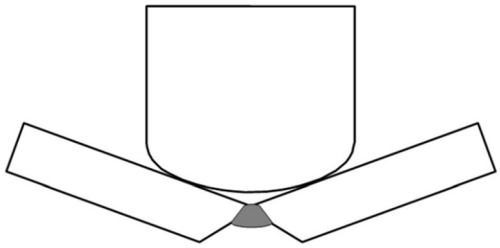

Fig. 5 Schematic illustration showing hinging effect in bend testing

3.5 Embrittlement vs weldability

The cold cracks present in hydrogenated steels are similar in nature to hydrogen-assisted cold cracking observed in weldments. It follows that embrittlement tests developed to produce cold cracks should likewise indicate susceptibility to hydrogen-assisted cold cracking in weldments. Embrittlement evaluations have the advantage of allowing the testing of small parts of the weldment without having to produce numerous welds under different loading conditions. It has the obvious disadvantage, however, of not exactly replicating the same thermo-mechanical or hydrogen diffusion conditions experienced in a weld.

The cooling conditions of temperature gradient, cooling rate, and hydrogen diffusion for embrittlement techniques compared to welds differ significantly. While cooling enables hydrogen diffusion out of the weldment during cooling, the quenching of the weld metal immediately after the welding ends stops the hydrogen movement and solid-state phase transformations. For example, the weldment in preparation for the bending test is first quenched in ice water and then placed in liquid nitrogen for storage until testing [31], which brings out the question of how cold storage modifies the weldment microstructure. Nevertheless, micromechanical embrittlement testing, such as the nano-indentation [42] and micro-cantilever [43] tests, enables the behaviour characterization of local microstructure (Fig. 7) as opposed to the general mean behaviour observed in weldability tests.

4 How test parameters affect test results

4.1 Effect of loading direction and history

The load is additive to the stress field so that greater load magnitudes induce greater local tensile stresses, favouring cracking. The direction in which load is applied to the weld, relative to the welding direction, will tend to favour one type of cold crack over the other. Cracks will preferentially grow in a direction oriented perpendicular to the load. Longitudinal loading, as experienced in G-BOP test, promotes transverse cracking while transverse loading as experienced in the M-WIC, Lehigh, and restraint circular weldability tests promotes cracking parallel to the welding direction.

The loading history will also tend to favour one type of cold crack over the other. As hydrogen diffuses and thermal stress builds up, the weldment susceptibility to cracking changes with time. Hence, the loading rate will generate a specific response for a specific metallurgical condition and subsequently the most susceptible microstructure to crack formation (Fig. 8).

4.2 Effect of stress

Stress has generally been taken to have the primary influence on HACC formation [3, 44]. Extensive weldability test data support this assumption, where higher applied stresses eventually lead to cracking. It has been demonstrated experimentally that a critical stress must be exceeded in order to cause

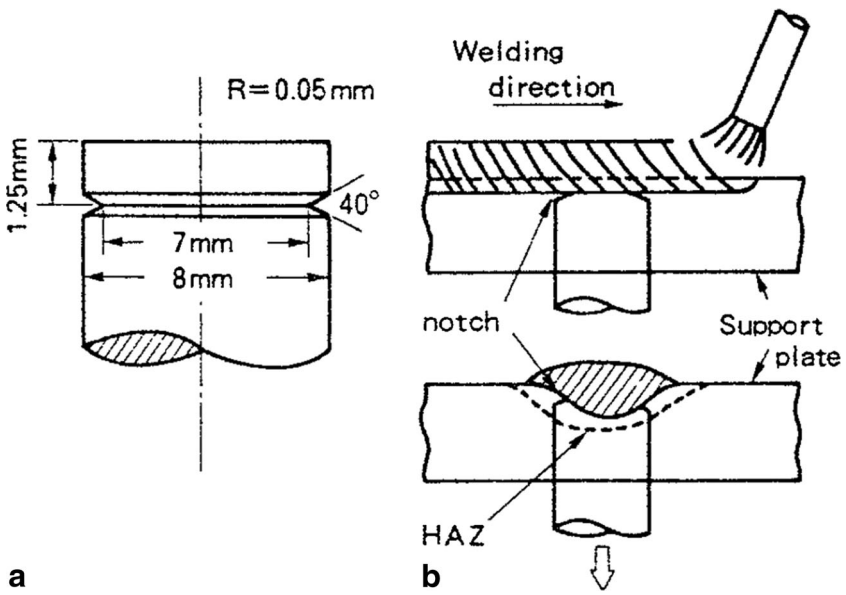

Fig. 6 Experimental set-up of **a** implant and **b** implant test [29]

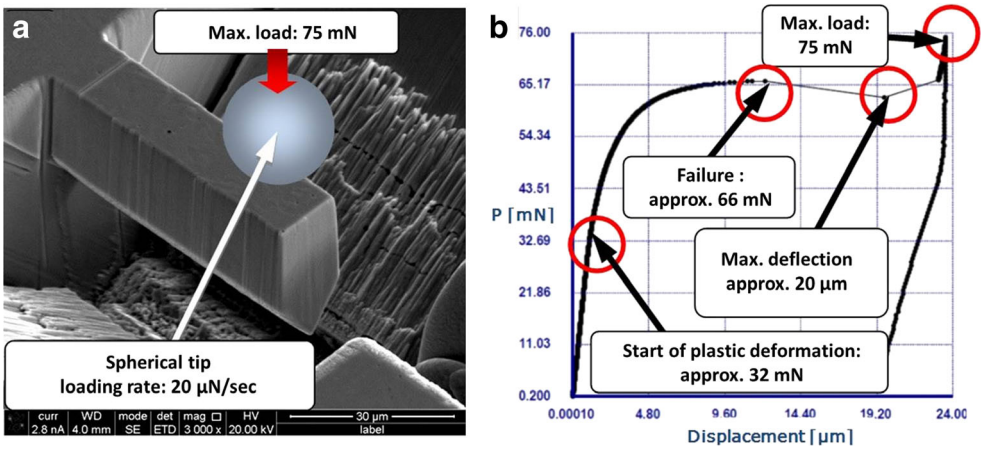

Fig. 7 **a** Micro-cantilever loaded with spherical nano-indent and **b** load–displacement (beam deflection) curve for acicular ferrite test specimen [43]

cracking. An important point to be made here is that, while stress is applied globally in weldability tests, it is actually the local stresses in the vicinity of each microstructural feature that are of primary importance to cracking models, and these stresses cannot be easily measured. Micromechanical tests [42, 43] permit to isolate the individual behaviour of a metallurgical feature contaminated by hydrogen and will help in understanding stress partitioning within the weldment.

When welding complex, multiple joint structures, residual stresses build that influence weldability. The presence of tensile stress formed during welding and cooling aggravates cracking. Along these lines, several weldability tests consist of applying a tensile load immediately after welding completion (e.g. TRC, implant test). This allows crack–no crack comparisons and permits a critical load to be measured, where greater critical loads indicate better weldability. In intrinsic tests, restraint hinders the free contraction of the weldment region, building up greater tensile stresses (Fig. 9). High loads add to the stresses normally associated with welding and result in greater local tensile strains. The upper limit of preload is bounded by the yield stress of the weldment.

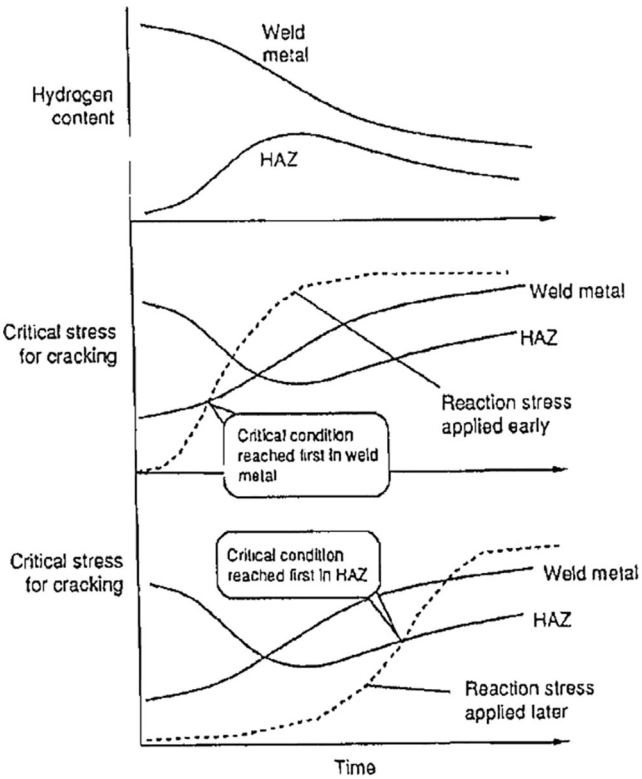

Fig. 8 Weldment response to different loading rates [2]

4.3 Effect of restraint

Restraint intensity is a measure of the resistance to strain after weld completion and can be thought of as a spring constant. It is influenced by the rigidity of the welding fixture as well as the weld coupon size and shape. The thermal and shrinkage stresses generated during and after welding interact with restraining forces to influence strain in the vicinity of the weldment. It is generally the case that high restraint gives high residual stress. Some weldability tests that involve the controlled variation of restraint intensity incorporate slots milled along the sides of the weld coupon (Lehigh U-groove test). Too small restraint levels, such as in the Schnadt-Fisco test, do not enable the HACC ranking of a wide range of weldment chemistries [6].

The H-slit restraint test consists of machining two test plates in a same larger plate and to control the restraint intensity by varying the slit length. The WIC and M-WIC tests have the tested plates welded onto an external fixture, the free-anchor welded lengths of the plates controlling the restraint intensity submitted to the weldment (Fig. 10). Reaction stresses in the weld metal develop earlier and attain a greater magnitude at higher restraint levels (Fig. 9). The restraint stress (σ_R in MPa) is expressed by

$$\sigma_R = \frac{SR_F}{h_w}, \tag{2}$$

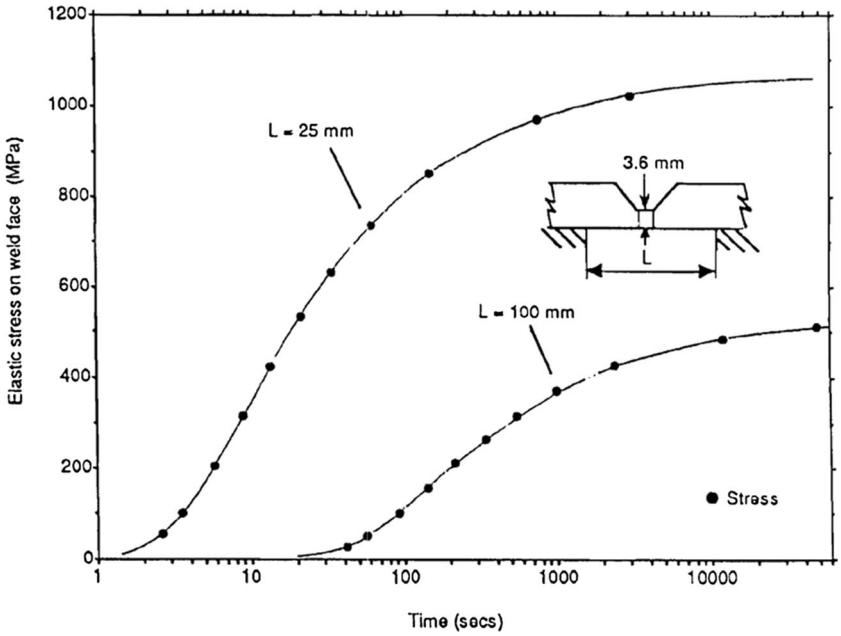

Fig. 9 Reaction stress estimated for two restraint lengths using a one-dimensional analysis [2]

where S is the total contraction (in mm), R_F is the tensile restraint intensity (in N mm^{-1} mm^{-1}), and h_w is the height of the weld metal throat (in mm).

Data from WIC testing [24] indicates that the maximum stress encountered in practice through restraint and bending is unlikely to exceed that imposed by the standard restraint length in the WIC test (16.4 kN mm^{-2} for 8.6-mm thick plate) and that restraint conditions are less critical than weld metal hydrogen content in inducing HACC. The traditionally used 25-mm restraint length provides a much higher restraint than that encountered during pipeline welding in the field. The M-WIC test

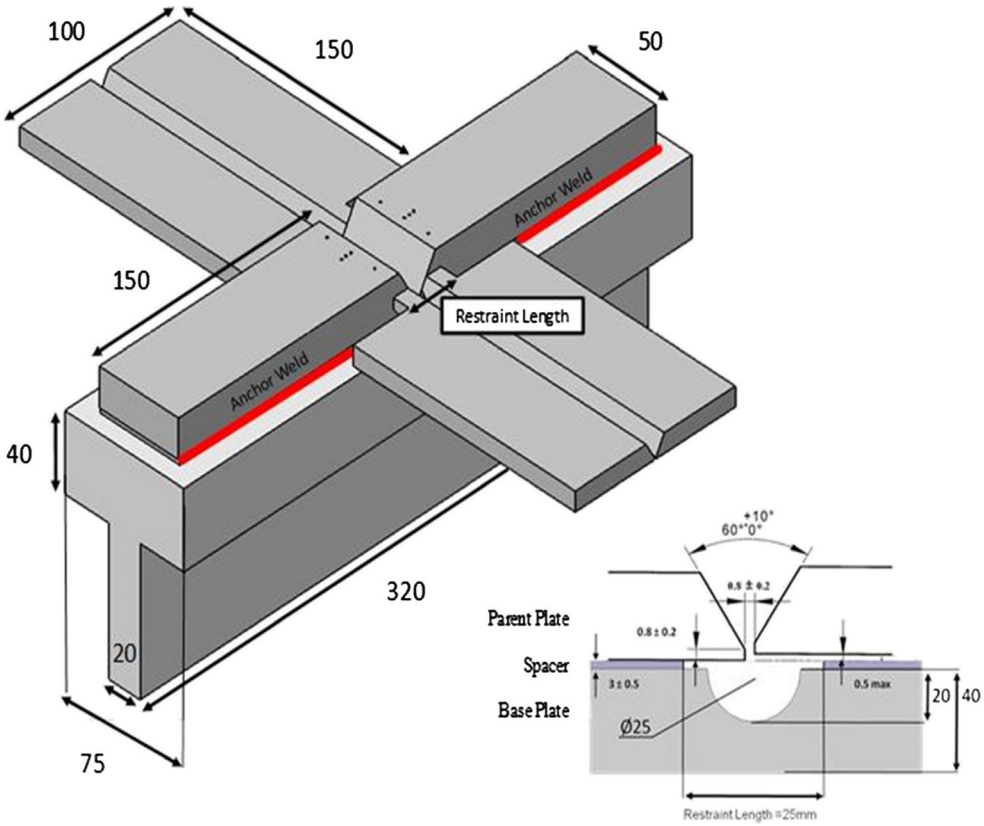

Fig. 10 Schematic illustration of M-WIC test [26]

was designed to conserve the restraint intensity–restraint length relationship while enhancing the evacuation of gases produced during electrode coating decomposition through the underneath 25-mm diameter groove.

It is of interest to note that several cold cracking weldability tests, such as circular patch and *t* tests, have been proven to generate weld solidification cracking too [45]. However, weldments highly susceptible to HACC are usually tested in low restraint conditions, which are known to favour solidification cracking [46]. Therefore, at small restraints, cold crack may possibly grow from pre-existing solidification cracks, which are identified by their dendritic fracture surface.

4.4 Effect of welding parameters

Welding parameters can have a significant impact on the cracking susceptibility of an alloy and hence must be considered when performing weldability tests. Ranking alloys for a given application should be done by using a similar welding process and parameters for both test and application when possible. However, the different thermal properties of some alloys may require higher current to achieve the same penetration. For this reason, it may be argued that alloys should be weldability tested each with unique welding parameters to produce a constant penetration. Whichever approach is chosen, it should be appreciated that any change in weld heat input can modify the size and shape of the weld and HAZ as well as change stress and strain behaviour. It can also change temperature gradients and cooling and solidification rates, which will result in different weld metal grain structures and sub-grain microstructures.

Welding heat input is defined as energy per unit length of weld and is commonly used for a comparative indication between welding conditions. Making welds with similar heat input for a given material provides roughly similar weld pool volumes and cooling rates, but not necessarily similar penetration and weld metal cross-sectional shape. Increasing heat input will increase the weld cross-section and lower the cooling rate. It is generally observed that reduced heat input gives greater susceptibility to cracking. Nevertheless, heat input is not sufficient information on its own as, for similar heat inputs and materials, lower arc voltages during shielded metal arc welding will deposit richer weld metal chemistries [7].

Yurioka and Kasuya [12] proposed a chart method to determine the necessary preheat temperature to avoid cracking in steel weld metals. This method is based upon master curves experimentally obtained for each set of welding conditions. The steel carbon equivalent value CEN is corrected depending on the weld metal hydrogen content (Fig. 11a), heat input, and CEIIW (Fig. 11b). This correction follows the enhancement of cold cracking at greater hydrogen levels and at smaller heat inputs. Once the corrected CEN value is obtained, the plate thickness is accounted for the minimum preheat temperature measured in a y-groove self-restraint cracking test (Fig. 11c). This preheat temperature determined in laboratory is corrected for welding practice in the field depending on steel yield strength (Fig. 11d).

4.5 Effect of preheat

The reduction of cracking by preheating (Fig. 12) has been proven to be of major interest for in-field construction, where restraint conditions are rarely changeable. A high and uniform preheating impacts the cracking susceptibility by slowing the cooling rate and subsequently enabling more hydrogen to diffuse away from the weldment region. Preheating may be performed by electrical resistance and oxy-flames on the joint and its surroundings. Uniform temperature in the joint region requires a certain delay between preheating finish and welding start, a rough estimation being 2-min waiting per 25-mm plate thickness. Combined preheating with low restraint designs is an efficient way in reducing cracking (Fig. 13)

The experimental data suggest a linear or logarithmic effect of hydrogen concentration on the critical preheat temperature to avoid cracking. The minimum preheat temperature T_{P1} has been estimated for preventing cracking in multiple-layer weld metals in GMAW [41] as a function of diffusible hydrogen content measured by the glycerol displacement method (H_{GL} in ml/100 g Fe), weld layer thickness (d_w in mm), and tensile strength of weld metal (σ_w in MPa). For $15<d_w<30$ mm, the equation is [47]

$$T_{P1} = 120 + 120\log\left(\frac{H_{\mathrm{GL}}}{3.5}\right) + 5(d_w{-}20) + 8(\sigma_w{-}83) \quad (3)$$

Okuda et al. proposed the following predictive equation for the necessary preheat temperature T_{P2} and interpass temperature for avoiding transverse weld metal HACC [47]:

$$T_{P2} = 6.03\sigma_{UTS} + 318.6\log(H_{GC}){-}554.3, \quad (4)$$

with σ_{UTS} the ultimate tensile strength of the weld metal (in MPa) and H_{GC} the weld metal hydrogen content measured by the gas chromatography method (in ml/100 g Fe).

The minimum preheat temperature is used to limit the cooling rate to an upper value. Even though the time for weld metal to cool from 800 to 500 °C ($t_{8/5}$) has been an effective indicator, the primary factor controlling weld

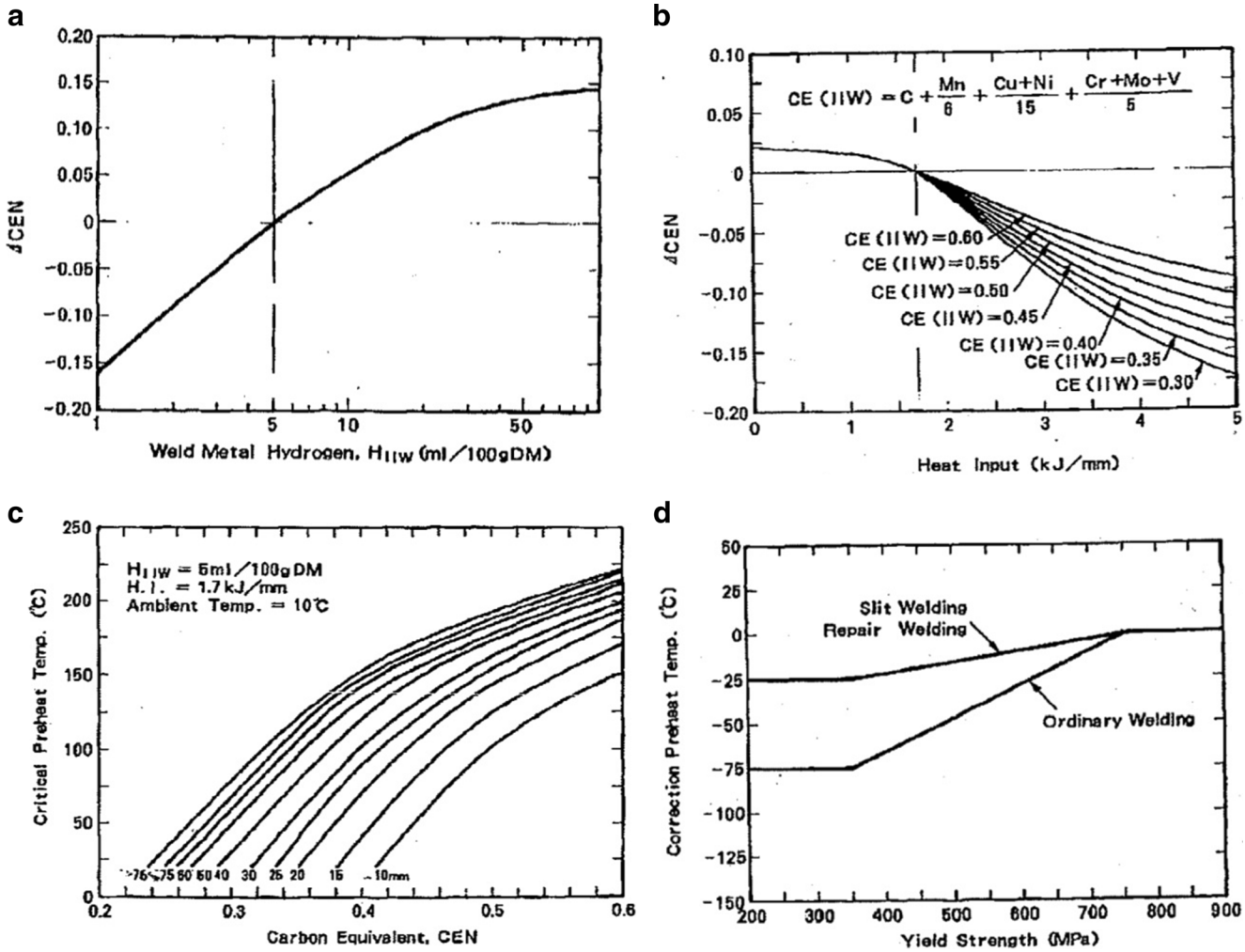

Fig. 11 Maps used in Yurioka's chart method for evaluating critical preheat temperature to avoid cracking for welding practice—**a** carbon equivalent (CEN) value correction as a function of weld metal hydrogen content, **b** CEN value correction as a function of welding heat input and carbon equivalent (CE_{IIW}) value, **c** critical preheat temperature for laboratory y-groove restraint testing as a function of plate thickness and CEN value at indicated test conditions, and **d** critical preheat temperature correction from laboratory test to welding practice as a function of steel yield strength [12]

metal cracking was hydrogen diffusion through control of the cooling time to 100 °C [48]. In WIC and gapped bead-on-plate tests, the cooling time to 100 °C ($t_{100,min}$ in s) depends on the carbon equivalent CEN value and the

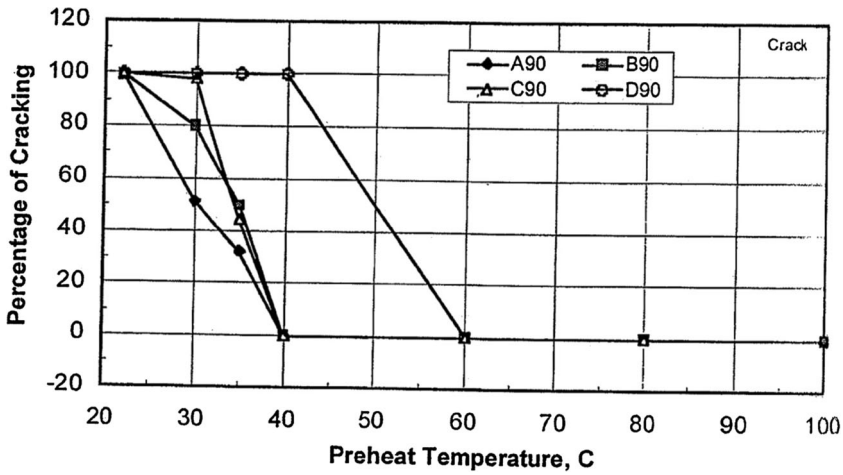

Fig. 12 Percentage of cracking as a function of preheat temperature for E9010 weld metal using WIC test [24]

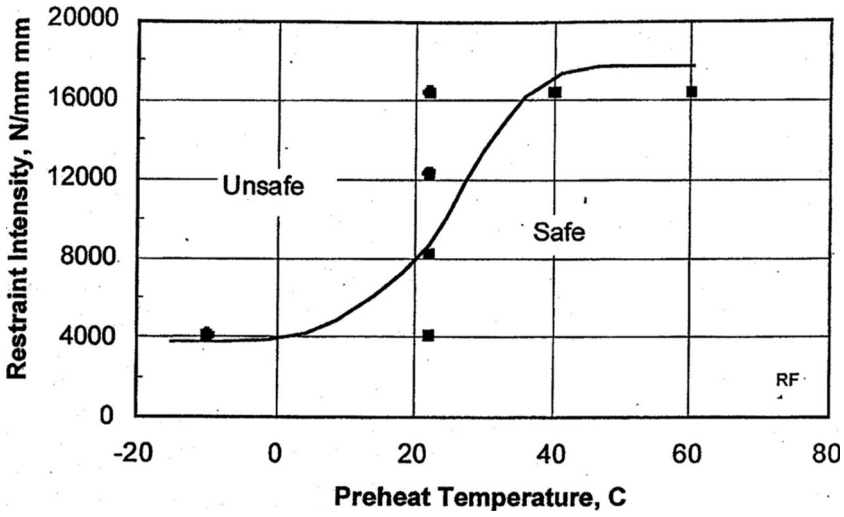

Fig. 13 Critical restraint intensity-preheat temperature map demarking cracking regions using WIC test [24]

diffusible hydrogen content H_d of the weld metal (in ml/100 g Fe):

$$t_{100,\min} = 34.1 \cdot (CEN) + \frac{H_d - 5}{3.5} - 9.1 \quad (5)$$

5 Measurements that uniquely define weldability

The desired outcome of weldability tests is cracking, which is most often quantified in percentage of weld length. It is usually assumed that for fixed testing conditions, an alloy having higher cracking susceptibility should result in a more extensive cracking in weldability tests. However, there are inherent problems when considering only crack length, due to alloy-dependent variations in thermal gradient and weld metal shape. Moreover, cracks may be embedded into the weldment and are thus difficult to characterize. In essence, the comparison of cracking extent becomes difficult for different alloys when all test conditions are not exactly the same.

A more appropriate measure of cracking susceptibility that is more characteristic of a particular alloy is its stress to fracture. Nevertheless, the fracture stress depends on the hydrogen level in the weldment region. Time to

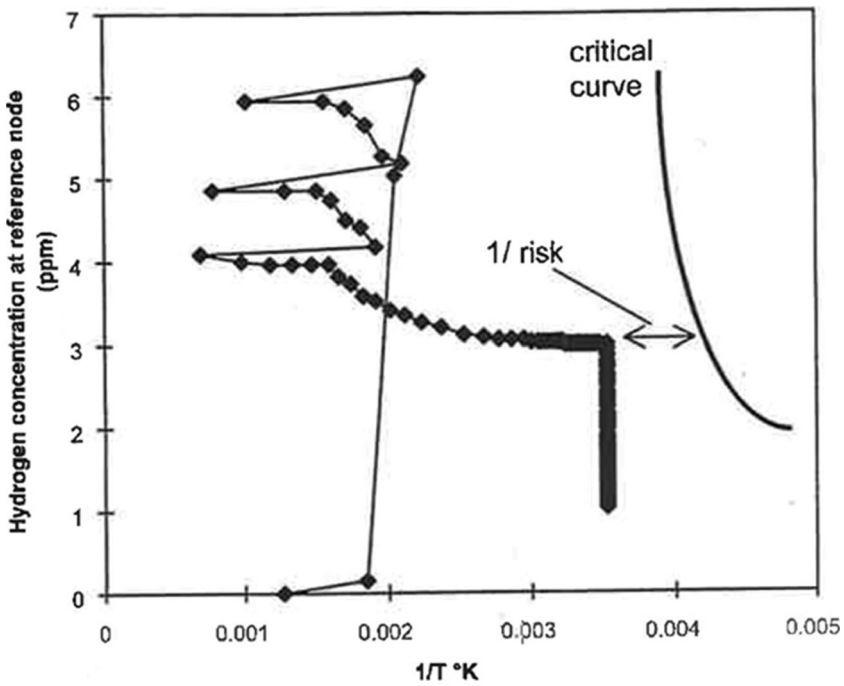

Fig. 14 Critical temperature–hydrogen map demarking region for cracking (*right side of the critical curve*) and compared to history of a multipass weld (*line with dots*) [53]

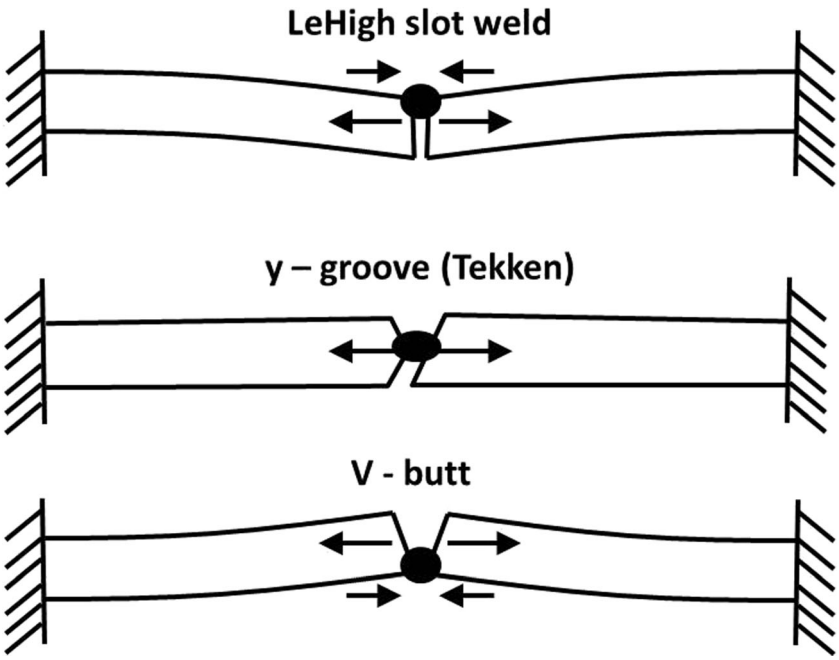

Fig. 15 Effect of weld eccentricity on local stress at weld root in different groove configurations [3]

fracture can also be viewed as a characteristic that defines weldability for a particular alloy, as alloys having higher crack susceptibility should fracture earlier after welding completion.

Cold cracking is caused by residual stresses after welding. Numerous weldability test designs have been developed to measure relative cracking behaviour of various alloys. Nevertheless, a better approach would be to consider weldability testing as experimental setups to identify critical conditions for cold crack initiation and growth mechanism. Mechanisms for both crack initiation and growth show stress and hydrogen to be controlling factors [49].

5.1 Diffusible hydrogen content

Diffusible hydrogen present in steel weldments limits the performance of the material. During arc welding processes, the dissociation of water molecules in the high-temperature arc plasma generates hydrogen ions that are absorbed by the liquid weld pool. In gas metal arc (GMA) welding, the use of

Groove Type	Kt	Groove Type	Kt
Oblique y	4.0	Single bevel-3	6.9
Double Vee	3.7	Single bevel-4	3.5
Single bevel-1	5.8	Symmetric Y	4.2
Single bevel-2	5.4		

Fig. 16 Stress concentration factor (K_t) at root of weld of basic joint geometry [34]

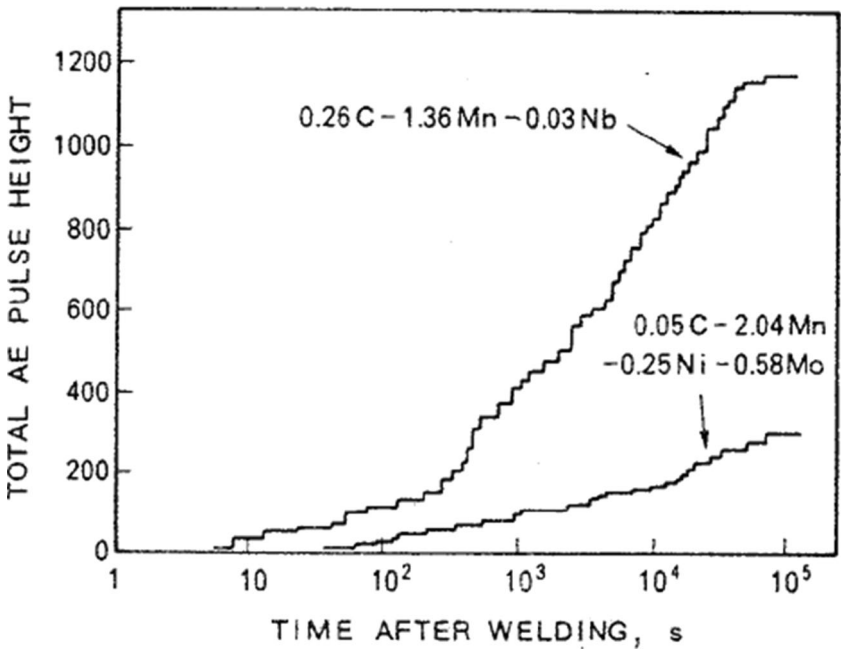

Fig. 17 Intermittent crack growth recorded by acoustic emission in Lehigh slot test [29]

dry inert gases protects the liquid pool from the contamination of atmospheric moisture. In the processes such as shielded metal arc welding (SMAW), flux-cored arc welding (FCAW), and submerged arc welding (SAW), a flux is used to prevent the molten metal from oxidation. Low hydrogen fluxes must be kept in a dry, warm environment to avoid moisture absorption and deposit weld metals with small hydrogen contents after baking the flux. Nevertheless, cellulosic coated electrodes have chemically bonded water ($-H_2O$) in their structure that enables fast deposition rates. In that case, hydrogen contents of the weldments can reach high levels (above 40 ml/100 g Fe) [50].

Despite the importance of hydrogen content in the weldment susceptibility to cracking, the hydrogen content of the weldment is not reported in the literature when performing weldability tests. This fact may be due to the difficulty in

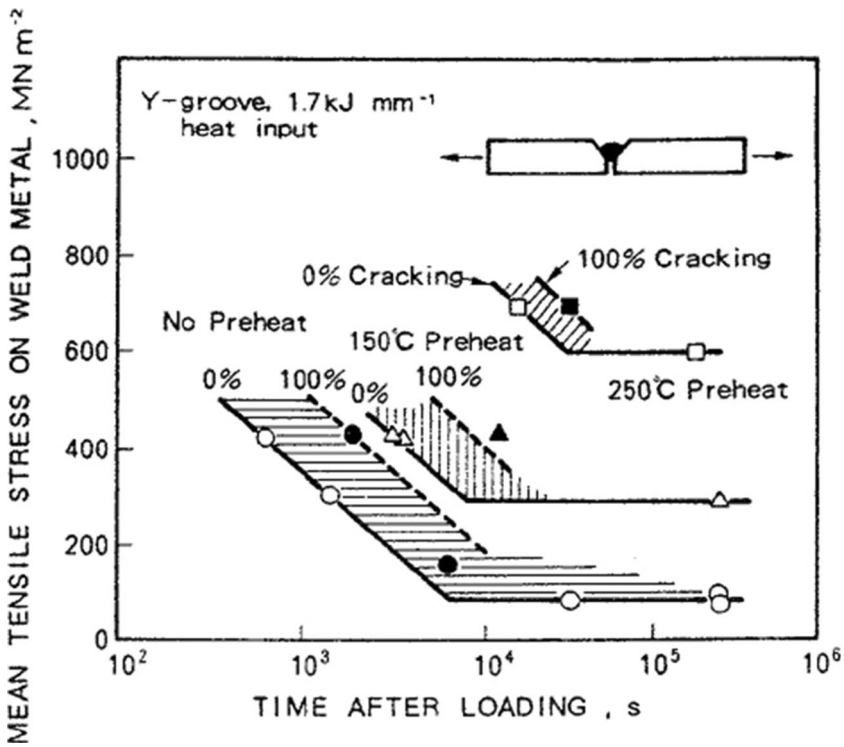

Fig. 18 Stress to fracture–time to failure relationship measured using tensile restraint cracking (TRC) test for a 700 MN.m^{-2} yield strength steel [3]

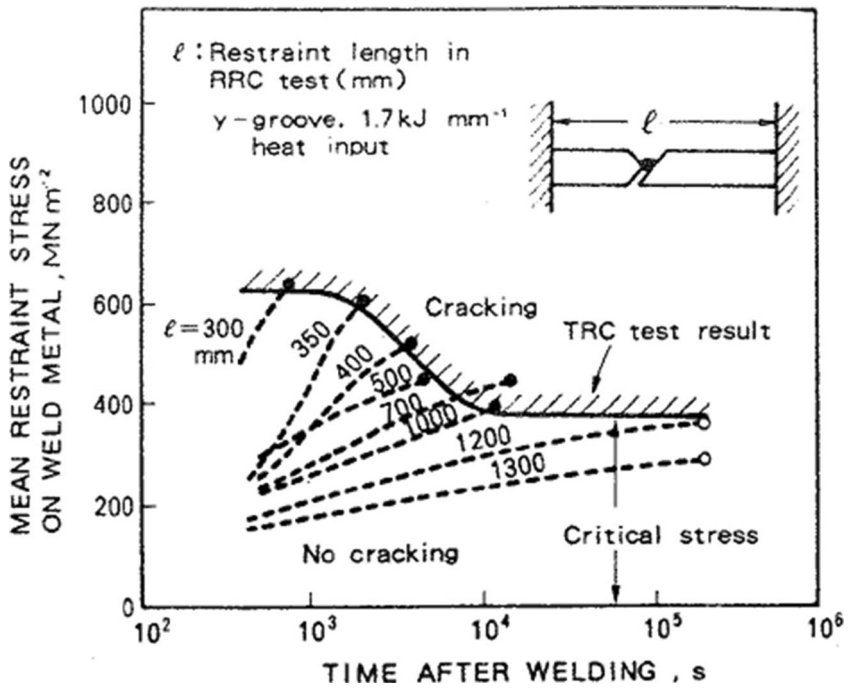

Fig. 19 Comparison RRC and TRC test results with y-groove configuration [3]

measuring diffusible hydrogen amount present in the weldment. Most popular methods include glycerin method, mercury method, and gas chromatography method. Each method gives different hydrogen values for a given weldment due to some absorption of hydrogen by the material of the method (such as glycerin) [50]. Hot extraction methods permit moreover to the total amount of hydrogen present in the weldment, to identify the trapping site by the temperature at which it releases hydrogen.

Statistical data modelling tools, used to evaluate the HACC susceptibility in weld metals, account for the hydrogen content in combination with the thermal history [51–53]. A probabilistic neural network method has been applied to estimate the hydrogen level and crack susceptibility of G-BOP tests of rutile flux-cored arc welds based upon consumable chemistries, welding process parameters, and environmental atmospheric conditions [37]. A holistic time-dependent model compares the crack driving forces at the crack tip with the material crack resistance, taking into account both the weld metal thermal history and hydrogen concentration, and was successfully applied to the pipeline front end welding operation [51, 52]. The local accumulation of hydrogen is quantified into the PHA cracking index as given by [40]:

$$PHA = -\log\left(\frac{[H]_{FB,cr}}{[H]_0}\right), \tag{6}$$

where $[H]_{\mathrm{FB,cr}}$ is the critical hydrogen concentration at the weld fusion line where a root crack initiates against the initial as deposited hydrogen concentration $[H]_0$. The value $[H]_{\mathrm{FB,cr}}$ is function of the weldment chemistry and the restraint level. Both hydrogen concentrations are expressed in ml/100 g Fe.

The weld metal hydrogen content and the thermal history affect the weld metal cracking susceptibility. Therefore, a critical temperature–hydrogen mapping concept was developed [53] to evaluate the risk of HACC formation in a multipass weld in Fig. 14. The left hand curve shows a plot of the local hydrogen content and the temperature during the complete history of welding. The right hand curve represents the critical hydrogen content for cracking and belongs to a family of such curves dependent upon the applied stress. The HACC susceptibility is calculated as the inverse of the distance separating the two curves (double arrow in Fig. 14), i.e. the inverse of the temperature difference between the actual weld metal temperature and the critical temperature for HACC as determined for a weld metal hydrogen content. The critical hydrogen content $[H]_c$ for HACC versus temperature, i.e. the right hand curve, can be represented by the equation

$$\log_{10}[H]_c = \log_{10}A - \frac{803}{T}, \tag{7}$$

where T is the absolute temperature (in K) and A is a constant determined by the external stress. A major drawback of this model is that it ignores the time factor, i.e. the incubation period to initiate a crack when exceeding a critical hydrogen amount.

5.2 Stress

Hydrogen-assisted cold cracking models view stress as important for the initiation and growth of a crack in a hydrogenated

Table 3 Checklist to be considered for each weldability test procedure

Category	Items
Alloy	Base metal – filler metal – dilution
Temperature	Cooling rate - preheat
Crack type	HAZ crack – weld metal crack
Time of cracking	Time after weld completion
Fracture mode	Intergranular – transgranular – cleavage
Test type	Intrinsic – extrinsic – bending – tensile
Load orientation	Longitudinal – transverse
Restraint	Coupon dimensions
Welding process	Process description
Welding parameters	Current – voltage – travel speed
Linear heat input	Heat input
Applied load	Maximum stress – loading rate
Hydrogen	Hydrogen content – atmospheric humidity
Local stress	Maximum strain – strain rate
Crack measurement	Percentage of weld length

microstructure [49]. Stress can be deduced from load and strain measurements. Measuring local strain in the vicinity of the weld during the welding cycle poses some unique challenges such as the high temperatures encountered in welding. The stress can be deduced from the deformation using the concept of restraint. The variation of stress distribution with the weld eccentricity and groove geometry (Fig. 15) has been considered using a concentration factor K_t for the stress calculation (Fig. 16). This multiplicative factor K_t is useful to compare welds deposited in grooves of different geometries.

5.3 Time of cracking

As HACC forms with some delay after welding completion, it is of interest to determine the time of fracture. A temperature-controlled tinting of the cracked areas can indicate the temperature at which the surface formed [6]. The intermittent crack growth has been confirmed experimentally. Acoustic emission sensors located near the weldment enable to follow the growth of the crack size [29] (Fig. 17). These sensors have proven the intermittent growth of cold cracking, suggesting that hydrogen transport to the crack tip is a critical requirement for HACC propagation.

The time of rupture shortens for greater stress, following experimental measurements using the implant test [4], TRC test [3], and RRC test [34]. While the TRC test applies post-welding a constant load transverse to the weld direction, the RRC test adjusts the transverse load to maintain a predefined local strain across the weld during cooling. The TRC and RRC results are in good correlation in terms of fracture stress and time to failure (Figs. 18 and 19). The characteristic delayed formation of cold cracking can be measured using a clip gauge positioned after weld completion across the weld metal [24], with a sudden increase in the strain value relating to the crack formation. Instrumenting the weldment surrounding regions with strain gauges enables to record the stress induced by the thermal contraction and solid phase transformation in the weldment and its sudden release by crack formation [36, 38].

6 Summary

Many weldability tests have been developed to rank cracking susceptibility of different alloys based solely upon relative comparisons of crack length. Although useful in making rough-cut rankings, a better approach is to consider weldability testing as an experimental means to identify critical conditions for hydrogen-assisted cold crack initiation and growth. Mechanisms for both crack initiation and growth show hydrogen and stress to be controlling factors, backed up by considerable experimental evidence. With advancing ideas regarding cracking mechanisms and improved testing methods, welding science is moving towards a point where the likelihood of cracking may someday be predicted for a given alloy and welding application. This paper has examined numerous weldability test approaches in order to identify important distinctions. Standardization of not only weldability test procedures but also defining what needs to be measured will help in the long-term understanding of alloy weldability. Table 3 is a proposed checklist of all the things one should consider and quantify, if possible, when performing weldability tests.

Acknowledgments The research work was funded by the Energy Pipeline CRC supported through the Australian Government's Cooperative Research Centres Program. The cash and in-kind support from the APIA-RSC is gratefully acknowledged.

References

1. Graville B (1986) A survey review of weld metal hydrogen cracking. Weld World 24(9/10):190–198
2. B.A. Graville (1995) Interpretive report on weldability tests for hydrogen cracking of higher strength steels and their potential for standardization. WRC Bull 400
3. Yurioka N, Suzuki H (1990) Hydrogen assisted cracking in c-mn and low alloy steel weldments. Int Mater Rev 35(4):217–249
4. Glover A and Rothwell B (1999) Specifications and practices for hydrogen crack avoidance in pipeline girth welds, In: First International Conference on Weld Metal Hydrogen Cracking in Pipeline Girth Welds, Wollongong, Australia, 13.1-13.18. WTIA
5. Kannengiesser T, Boellinghaus T (2013) Cold cracking tests—an overview of present technologies and applications. Weld World 57:3–37

6. North TH, Rothwell AB, Glover AG, and Pick RJ (1982) Weldability of high strength line pipe steels. Weld J, August, 243s-257s
7. Coniglio N, Linton V, Gamboa E (2010) Coating composition, weld parameter, and consumable conditioning effects on weld metal composition in shielded metal arc welding. Sci Technol Weld Join 15(5): 361–368
8. Natalie CA, Olson DL, Blander M (1986) Physical and chemical behavior of welding fluxes. Annu Rev Mater Sci 16:389–413
9. Coniglio N, Barbaro F, Linton VM, Gamboa E, and Kurji R (2010) Hydrogen assisted cold cracking susceptibility of weld metal deposited by cellulosic shielded metal arc welding consumables. In: Proceedings of the 8th International Pipeline Conference, IPC2010, Calgary, Canada. IPC2010-31680
10. Hart P (1986) Effects of steel inclusions and residual elements on weldability. Met Constr, October, 610–616
11. Talas S (2010) The assessment of carbon-equivalent formulas in predicting the properties of steel weld metals. Mater Des 31(5): 2649–2653
12. Yurioka N, Kasuya T (1995) A chart method to determine necessary preheat in steel welding. Weld World 35(5):327–334
13. Dearden J, O'Neil H (1940) A guide to the selection and welding of low alloy structural steels. Trans Int Weld 3(10):203–214
14. Suzuki H, Tamura H (1961) Weldability of high strength steels evaluated by synthetic HAZ ductility test. Rep NRIM 3(1):47–59
15. Hannerz NE (1980) The influence of silicon on the weldability of mild and high tensile structural steel, IIW Doc. IX-1169-80
16. Uwer D and Hohne H (1991) Determination of suitable minimum preheating temperatures for the cold-crack-free welding of steels, IIW Doc. IX-1631-9
17. Itoh Y, Bessho K (1968) Cracking parameter of high strength steels related to HAZ cracking. J Jpn Weld Soc 37(9):983–989
18. Duren C (1985) Equations for the prediction of cold cracking in field-welding large diameter pipes, IIW Doc. IX-1356-85
19. Graville BA Cold cracking in welds in HSLA steels, Proc. Conf. on Weldability of HSLA Structural Steel, Rome, ASM
20. Yurioka N, Ohshita S, Tamehiro H (1981) Study on carbon equivalents to assess cold cracking tendency in steel welding. AWRA Symposium on Pipeline Welding in the 80's, Melbourne
21. Lazor RB and Graville BA (1983) Effect of microalloying on weld cracking in low carbon steels. Can Welder and Fabricator, July, 21–23
22. Kasuya T, Yurioka N (1995) Determination of necessary preheat temperature to avoid cold cracking under varying ambient temperature. ISIJ Int 35(10):1183–1189
23. Kou S (2002) Welding metallurgy, 2nd edn. Wiley, New York
24. Alam N, Dunne D, and Barbaro F (1999) Weld metal crack testing for high strength cellulosic electrodes. In: First International Conference on Weld Metal Hydrogen Cracking in Pipeline Girth Welds, Wollongong, Australia, 9.1-9.23. WTIA
25. Signes EG, Howe P (1988) Hydrogen-assisted cracking in high-strength pipeline steels. Weld J 67(8):163s–170s
26. Kurji R, Griggs J, Linton V, Kotousov A, Gamboa E, Ghomashchi R, and Coniglio N (2013) An improved welding Institute of Canada test for evaluation of high strength pipeline steel weldability. In: Proc. 6th Pipeline Technology Conference, Ostend
27. Magudeeswaran G, Balasubramanian V, Madhusudhan Reddy G (2008) Hydrogen induced cold cracking studies on armour grade high strength, quenched, and tempered steel weldments. Int J Hydrog Energy 33:1897–1908
28. Sawhill JM Jr, Dix AW, Savage WF (1974) Modified implant test for studying delayed cracking. Weld J 53(13):554s–560s
29. Vasudevan R, Stout RD and Pense AW (1981) Hydrogen-assisted cracking in HSLA pipeline steels, Weld J, Sept, 155s-168s
30. Beachem CD (1972) A new model for hydrogen-assisted cracking (Hydrogen "Embrittlement"). Metall Trans 3:437–451
31. Law M, Nolan D, Holdstock R (2008) Method for the quantitative assessment of transverse weld metal hydrogen cracking. Mater Charact 59:991–997
32. Peterneder E and Königshofer H (1999) Capabilities and limitations of cellulosic electrodes—a producer's perspective. In: First International Conference on Weld Metal Hydrogen Cracking in Pipeline Girth Welds, Wollongong, Australia, 17.1-17.17. WTIA
33. Sarrafan S, Ghaini FM and Rahimi E (2010) Weld metal hydrogen cracking in transmission pipelines construction, In: Proceedings of the 8th International Pipeline Conference IPC2010, Calgary, Canada. IPC2010-31240
34. Alam N, Dunne D, Squires I, Barbaro F and Feng B (1996) Weldment cold cracking—the effect of hydrogen and other factors, In: Proceedings of Joint Seminar Hydrogen Management in Steel Weldments, Melbourne, Australia, 49–60. WTIA
35. Kinsey AJ. The welding of structural steels without preheat, Weld J, 79 (4), 79s-88s
36. Graville BA, McParlan M (1974) Weld-metal cold cracking. Met Constr Br Weld J 6(2):62–63
37. Sterjovski Z, Pitrun M, Nolan D, Dunne D, Norrish J (2007) Artificial neural networks for predicting diffusible hydrogen content and cracking susceptibility in rutile flux-cored arc welds. J Mater Process Technol 184:420–427
38. McParlan M, Graville BA (1976) Hydrogen cracking in weld metals. Weld J 55(4):95s–102s
39. Vasudevan R, Stout RD, Pense AW (1980) A field weldability test for pipeline steels—part I. Weld J 59(3):76s–84s
40. Suzuki H, Yurioka N, Okumura M (1983) A new cracking parameter for welded steels considering local accumulation of hydrogen. Weld World 21(5/6):110–132, Doc. IIS/IIW-755-83
41. Ushio M, Sugitani Y, Kanayama K, Aida I, Hara N and Nakano T (1999) Cracking in GMAW pipeline girth welds based on experiences in pipeline construction in Japan, in: First International Conference on Weld Metal Hydrogen Cracking in Pipeline Girth Welds, Wollongong, Australia, 10.1-10.19. WTIA
42. Katz Y, Tymiak N, Gerberich WW (2001) Nanomechanical probes as new approaches to hydrogen/deformation interaction studies. Eng Fract Mech 68(6):619–646
43. Costin WL, Lavigne O, Linton V, Brown IH, Kotousov AG, Barbaro FJ and Ghomashchi R (2013) Micromechanical examination of the relationship between weld metal microstructure and hydrogen assisted cold cracking, In: Proc. 6th Pipeline Technology Conference, Ostend
44. Bailey N (1994) Weldability of ferritic steels. Abington Publishing
45. Lippold JC (2005) Recent developments in weldability testing. In: Hot cracking phenomena in welds, Springer: 271–290
46. Cross CE, Boellinghaus T (2006) The effect of restraint on weld solidification cracking in aluminium. Weld World 50:51–54
47. Yurioka N (1999) Predictive methods for prevention and control of hydrogen assisted cold cracking, In: First International Conference on Weld Metal Hydrogen Cracking in Pipeline Girth Welds, Wollongong, Australia, 2.1-2.16. WTIA
48. Barbaro FJ (1999) Types of hydrogen cracking in pipeline girth welds, In: First International Conference on Weld Metal Hydrogen Cracking in Pipeline Girth Welds, Wollongong, Australia, 11.1-11.15. WTIA
49. Hirth JP (1980) Effect of hydrogen on the properties of iron and steel. Metall Trans 11A:861–890
50. Padhy GK, Komizo Y (2013) Diffusible hydrogen in steel weldments. Trans JWRI 42:39–62
51. Fletcher L, Yurioka N (2000) A holistic model of hydrogen cracking in pipeline girth welding. Weld World 44(2):29–36

52. Fletcher L and Yurioka N (1999) A holistic model of hydrogen cracking in pipeline girth welding, In: First International Conference on Weld Metal Hydrogen Cracking in Pipeline Girth Welds, Wollongong, Australia, 12.1-12.14. WTIA

53. A. Glover and B. Graville (1999) The risk of hydrogen cracking in multipass welds and its effect upon procedure design, In: First International Conference on Weld Metal Hydrogen Cracking in Pipeline Girth Welds, Wollongong, Australia, 9.1-9.23. WTIA